

**Title:** The relationship between major symptoms in *Eimeria tenella* early infection time and the disruption of intestinal barrier function via altering gene expression of epithelial junctional molecules in the cecum

## **HIGHLIGHTS**

- Diarrhea by *E. tenella* infection causes by junctional barrier's disruption.
- Higher expression of claudin-2 related with diarrhea in *E. tenella* infected chicks.
- Several junctional molecules relate with bleeding by *E. tenella* infection.

1  
2  
3  
4  
5  
6  
7  
8  
9  
10  
11  
12  
13  
14  
15  
16  
17  
18  
19  
20  
21  
22  
23  
24  
25  
26  
27  
28  
29  
30  
31  
32  
33  
34  
35  
36  
37  
38  
39  
40  
41  
42  
43  
44  
45  
46  
47  
48  
49  
50  
51  
52  
53  
54  
55  
56  
57  
58  
59  
60  
61  
62  
63  
64  
65

1 **Title:** Relationship between *Eimeria tenella* associated-early clinical signs and molecular  
2 changes in the intestinal barrier function.

3  
4 **Running title:** *Eimeria tenella*'s infection effects on epithelial junctional molecules' gene  
5 expression.

6  
7 **Authors:** Hung Hoang Son Pham<sup>1</sup>, Makoto Matsubayashi<sup>2</sup>, Naotoshi Tsuji<sup>3</sup>, and Toshimitsu  
8 Hatabu<sup>1,\*</sup>

9  
10 **Author address:**

11 <sup>1</sup>Laboratory of Animal Physiology, Graduate School of Environmental and Life Science,  
12 Okayama University, 1-1-1 Tsushima-Naka, Kita-Ku, Okayama 700-8530, Japan.

13 <sup>2</sup> Department of Veterinary Science, Graduate School of Life and Environmental Sciences,  
14 Osaka Prefecture University, Izumisano, Osaka 598-8531, Japan.

15 <sup>3</sup> Department of Molecular and Cellular Parasitology, Kitasato University Graduate School of  
16 Medical Science, 1-15-1 Kitasato, Minami-ku, Sagamihara 252-0374, Japan.

17  
18 **\*Correspondence to** Toshimitsu HATABU, Ph. D., Laboratory of Animal Physiology, Graduate  
19 School of Environmental and Life Science, Okayama University, 1-1-1 Tsushima-Naka, Kita-  
20 Ku, Okayama 700-8530, Japan. TEL: +81-86-251-8306, FAX: +81-86-251-8388, E-mail:  
21 hatabu@okayama-u.ac.jp.

1  
2  
3  
4 **22 Abstract**

5  
6  
7 **23 The major clinical signs of coccidiosis in chickens due to *Eimeria* parasite are diarrhea and**  
8  
9 **24 bloody feces. Previous studies showed that the impairment of the intestinal epithelial barrier and**  
10  
11 **25 the elevation of the intestinal permeability are causes of clinical signs associated with coccidia**  
12  
13 **26 challenges. Nevertheless, the information about molecular changes of the epithelial barrier at the**  
14  
15 **27 early stage of the infection with a specific *Eimeria* species has not been mentioned. Hence, this**  
16  
17 **28 study aims to elucidate the temporal relationships between epithelial barrier conditions and**  
18  
19 **29 clinical signs in chickens infected with *Eimeria tenella* over the time from the earliest stages of**  
20  
21 **30 infection.**

22  
23  
24  
25  
26  
27 **31 White Leghorn chickens were inoculated with  $1 \times 10^4$  oocysts of *E. tenella*. Thereafter the**  
28  
29 **32 chickens were monitored for their daily clinical signs through observation, and between 5 dpi to**  
30  
31 **33 10 dpi, feces were collected for oocysts counting. Chickens were then administrated with**  
32  
33 **34 fluorescein isothiocyanate-dextran (FITC-d) for gastrointestinal permeability test and tissues**  
34  
35 **35 were collected each day for histopathological observation and total RNA extraction. Finally, the**  
36  
37 **36 mRNA expression levels of the tight and adherens junction genes and cytokine genes were**  
38  
39 **37 evaluated using the quantitative real-time polymerase chain reaction (qRT-PCR).**

40  
41  
42  
43  
44 **38 In this study, clinical signs such as diarrhea and bloody feces were observed concurrently**  
45  
46 **39 from 3 to 8 dpi. Histopathology changes such as severe inflammation, hemorrhage, and epithelial**  
47  
48 **40 desquamation were identified in the cecum specimens. The FITC-d level in the *E. tenella*-**  
49  
50 **41 infected group was significantly higher than in the control group. In the infected group, the**  
51  
52 **42 expression of claudin-2 gene was also upregulated, whereas the expressions of claudin-3 and E-**  
53  
54 **43 cadherin genes were decreased as compared to the control group. These results implied that**  
55  
56  
57  
58  
59  
60  
61  
62  
63  
64  
65

1  
2  
3  
4  
5  
6  
7  
8  
9  
10  
11  
12  
13  
14  
15  
16  
17  
18  
19  
20  
21  
22  
23  
24  
25  
26  
27  
28  
29  
30  
31  
32  
33  
34  
35  
36  
37  
38  
39  
40  
41  
42  
43  
44  
45  
46  
47  
48  
49  
50  
51  
52  
53  
54  
55  
56  
57  
58  
59  
60  
61  
62  
63  
64  
65

44 **clinical signs** of avian coccidiosis were associated with the intestinal barrier disruption via  
45 changes in expression levels of claudins and E-cadherin at the intestine.

46

47 **Keywords:** adherens junction; bloody **feces**; diarrhea; *Eimeria tenella*; epithelial barrier; tight  
48 junction.

1  
2  
3  
4 **49 Introduction**

5  
6  
7 50 Avian coccidiosis is a pathogenic disease in poultry that is caused by intracellular  
8  
9  
10 51 apicomplexan parasites belonging to several different *Eimeria* species closely related to human  
11  
12 52 enteric pathogens, such as *Cryptosporidium* spp. (Dalloul and Lillehoj, 2006). Four *Eimeria*  
13  
14 53 species, *Eimeria acervulina*, *E. necatrix*, *E. maxima*, and *E. tenella* are the most frequent species  
15  
16 54 in the chicken (Adriana et al., 2013). Each of these parasites infects a specific place in the  
17  
18  
19 55 intestines. This protozoan parasite exhibits a complex life cycle comprising both extracellular  
20  
21  
22 56 and intracellular stages. After ingesting the sporulated oocysts (exogenous stage of this parasite)  
23  
24 57 containing the invasive form (sporozoite), sporozoites are released and invade the intestinal  
25  
26  
27 58 epithelial cells. The intracellular stage (endogenous stage) then occurs inside the host intestine's  
28  
29  
30 59 epithelial cells, which involves schizogony (asexual reproduction) followed by gametogony  
31  
32 60 (sexual stage). *Eimeria tenella* specifically infects the paired ceca in chickens and causes  
33  
34 61 extensive bleeding. The symptoms such as bleeding and malabsorption by *E. tenella* infection  
35  
36  
37 62 are caused by the destruction of epithelial cells and small blood vessels in lamina propria when  
38  
39 63 the merozoites are released from second-generation schizonts (El-Ashram et al., 2019). Severe  
40  
41 64 tissue damage occurs in the chick after parasite proliferation begins (Estela et al., 2015). When  
42  
43  
44 65 the merozoites are released from the second-generation schizont-infected epithelial cells, the  
45  
46 66 parasites destroy the tissues, including micro-vessels, around the infected cells. As a result,  
47  
48  
49 67 several clinical signs such as diarrhea, bloody feces, and reduced body weight are observed,  
50  
51 68 resulting in severe economic losses in the poultry industry (Burrell et al., 2019; Reid et al.,  
52  
53 69 2014).

54  
55  
56 70 The intestinal epithelial layer forms the major barrier from the external environment and  
57  
58 71 plays an essential role in food digestion and nutrient absorption. (Groschwitz & Hogan, 2009;  
59  
60  
61  
62  
63  
64  
65

1  
2  
3  
4 72 Lechuga et al., 2017). The intestinal epithelial barrier integrity is maintained by intercellular  
5  
6 73 junction molecular complexes, including tight and adherens junctions. Intestinal epithelial cells  
7  
8 74 are connected strongly by tight junction proteins such as claudins (CLDNs), occludin (OCDN),  
9  
10 75 and zonula occludins (ZO) at their apical ends. These proteins are involved in paracellular  
11  
12 76 pathway formation that regulates the passages of ions, solutes, and water in adjacent intercellular  
13  
14 77 spaces (Hossain and Hirata, 2008; Odenwald & Tuner, 2017). Adherens junction molecules are  
15  
16 78 involved in strong adhesive bonds between the epithelial cells and intercellular communications  
17  
18 79 (Chida et al., 2009). Therefore, disruption of the intestinal barrier complex is closely associated  
19  
20 80 with the alterations of tight and adherens junction molecules, which affects the paracellular  
21  
22 81 permeability that contributes to gastrointestinal clinical signs such as diarrhea (Awad et al.,  
23  
24 82 2017; Chow et al., 2011).

25  
26  
27  
28  
29  
30  
31 83 Although the clinical signs of avian coccidiosis and the life cycle of *Eimeria* have been  
32  
33 84 well studied, there are a few studies conducted to investigate the relationship between the  
34  
35 85 molecular basis of the gut barrier dysfunction and the *Eimeria* infection. Chen et al. (2015) has  
36  
37 86 reported that increased certain cytokines and decreased OCDN induce the gut barrier failure and  
38  
39 87 inflammation in jejunum mucosa of broilers, resulting in elevated levels of endotoxin and acidic  
40  
41 88 glycoprotein in the chick serum. Teng et al. (2020) have shown that gene expression of CLDN-1  
42  
43 89 and Junctional adhesion molecule (JAM)-2 was linearly upregulated by challenge infection of  
44  
45 90 mixed *Eimeria* spp in the jejunum at 6 days post-infection (dpi). These studies evaluated the  
46  
47 91 phenomenon of attack infection against chickens administrated with three coccidia (*E.*  
48  
49 92 *acervulina*, *E. maxima*, and *E. tenella*) mixture vaccine. Although *Eimeria* parasites have organ  
50  
51 93 specificity, it cannot be denied that vaccination with three parasite species mixture can affect  
52  
53 94 each other. Therefore, it is difficult to accurately observe the phenomenon caused by only *E.*

1  
2  
3  
4  
5  
6  
7  
8  
9  
10  
11  
12  
13  
14  
15  
16  
17  
18  
19  
20  
21  
22  
23  
24  
25  
26  
27  
28  
29  
30  
31  
32  
33  
34  
35  
36  
37  
38  
39  
40  
41  
42  
43  
44  
45  
46  
47  
48  
49  
50  
51  
52  
53  
54  
55  
56  
57  
58  
59  
60  
61  
62  
63  
64  
65

95 *tenella* infection in the chick cecum. For this reason, our study has only focused on the *E. tenella*  
96 infection at the chick cecum. This study aims to clarify the relationship between the status of  
97 intestinal epithelial junctional molecules and the typical clinical signs of chicken infected with *E.*  
98 *tenella* throughout the infection's development. The relationships between clinical signs of *E.*  
99 *tenella* infection and the changes in gene expressions of intercellular junction molecules have  
100 been investigated throughout the time course of the infection, especially at the early stage.  
101 Besides, expression levels of pro-inflammatory cytokines that can modulate the expression of  
102 intestinal junction proteins have also been evaluated.

1  
2  
3  
4  
5  
6  
7  
8  
9  
10  
11  
12  
13  
14  
15  
16  
17  
18  
19  
20  
21  
22  
23  
24  
25  
26  
27  
28  
29  
30  
31  
32  
33  
34  
35  
36  
37  
38  
39  
40  
41  
42  
43  
44  
45  
46  
47  
48  
49  
50  
51  
52  
53  
54  
55  
56  
57  
58  
59  
60  
61  
62  
63  
64  
65

## 103 **Materials and Methods**

### 104 **Parasite**

105 The *E. tenella* NIAH strain which is virulent and maintained at the Laboratory of Animal  
106 Physiology in Okayama University (Okayama, Japan) was used. *E. tenella* oocysts were purified  
107 by the sugar flotation method, sporulated at 28°C in 2.5% potassium dichromate, and stored at  
108 4°C before use.

### 110 **Animals, tissue collection, and experimental design**

111 Eggs (White Leghorn) were purchased from **Kui** potory Co., Ltd. (Mihara, Japan). Eggs  
112 were incubated at  $37.7 \pm 1^\circ\text{C}$  until hatching. After hatching, chicks were maintained at the  
113 coccidian-free room, fed, and watered *ad libitum*. The chicks were housed at a constant  
114 temperature ( $27 \pm 1^\circ\text{C}$ ) with a 12 h dark/light cycle. All procedures were approved by the  
115 Animal Care and Use Committee, Okayama University (OKU-2018561) and were conducted  
116 following the Policy on the Care and Use of the Laboratory Animals, Okayama University.

117 The chicks (n = 45) were randomly divided into three groups: Control group, chicks in  
118 this group were not treated as a control; Fasting group, chicks in this group fasted 24 h before the  
119 test as a positive control; and *E. tenella* group, chicks in this group were inoculated with mature  
120 sporulated oocysts of *E. tenella* ( $1 \times 10^4$  oocysts/chick) at 14 days old. Three chicks were  
121 randomly picked up and anesthetized using Pentobarbital sodium salt (Tokyo Chemical Industry  
122 Co., Ltd., Tokyo, Japan), and sacrificed by cervical dislocation for cecum collection until 6 dpi.  
123 One of the ceca was immediately frozen at  $-80^\circ\text{C}$  for gene expression analysis and a second one



1  
2  
3  
4  
5  
6  
7  
8  
9  
10  
11  
12  
13  
14  
15  
16  
17  
18  
19  
20  
21  
22  
23  
24  
25  
26  
27  
28  
29  
30  
31  
32  
33  
34  
35  
36  
37  
38  
39  
40  
41  
42  
43  
44  
45  
46  
47  
48  
49  
50  
51  
52  
53  
54  
55  
56  
57  
58  
59  
60  
61  
62  
63  
64  
65

124 was separated three pieces (proximal, medial, and distal regions). Each of the tissue pieces was  
125 fixed with 10% formaldehyde for histopathological observation.

126

127 **Fecal collection and oocysts counting**

128 We sampled feces daily from 5 to 10 dpi for oocysts counting. Oocysts per gram of  
129 feces were counted by the fecal flotation method using a saturated sucrose solution (Ho et al.,  
130 2021). Briefly, fecal samples (2 g/tube) were mixed thoroughly with 10 ml of distilled water,  
131 followed by 2,500 rpm centrifuging for 5 minutes at room temperature. The supernatant then was  
132 discarded, and 10 ml of the saturated sucrose solution was added to the tubes, mixed thoroughly,  
133 and centrifuged at 2,500 rpm for 5 minutes at room temperature. The supernatant was transferred  
134 to another 15 ml centrifuge tubes and mixed well. The supernatant (10 µl) was dropped on the  
135 slide glass, covered with cover glass, and the oocysts were counted using light microscopy  
136 (triplicate/tube).

137

138 **Histopathological observation**

139 The middle part of formaldehyde-fixed ceca was removed and embedded in paraffin,  
140 sectioned at 6 µm thickness, and de-paraffinized. We stained the sectioned specimens using a  
141 hematoxylin-eosin (HE) solution. HE specimens (6 specimens/chick, 200 µm interval) were  
142 observed under the light microscope (Olympus FSX100, Olympus, Tokyo, Japan) to evaluate the  
143 histological score (magnification, × 200). The inflammation levels of ceca were evaluated using  
144 a 0 to +4 scoring system described previously (Table 1; Erben et al., 2014).

145

1  
2  
3  
4  
5  
6  
7  
8  
9  
10  
11  
12  
13  
14  
15  
16  
17  
18  
19  
20  
21  
22  
23  
24  
25  
26  
27  
28  
29  
30  
31  
32  
33  
34  
35  
36  
37  
38  
39  
40  
41  
42  
43  
44  
45  
46  
47  
48  
49  
50  
51  
52  
53  
54  
55  
56  
57  
58  
59  
60  
61  
62  
63  
64  
65

**146 Measurement of intestinal permeability**

147 To evaluate the permeability levels in the intestine, the plasma level of fluorescein  
148 isothiocyanate-dextran (FITC-d; MW 4,000 Da; Sigma-Aldrich Co., St. Louis, MO) was  
149 determined as described by Kuttappan et al. (2015). Briefly, FITC-d was orally administrated to  
150 chicks (from day 2<sup>nd</sup> to 6<sup>th</sup> dpi) in all groups. One hundred fifty minutes later, peripheral blood  
151 samples were collected from a cardiac puncture in each chick used 0.2 ml anticoagulant (Heparin  
152 sodium injection 10,000U/10 ml, AY Pharmaceuticals Co., Ltd., Tokyo, Japan) /chick, mix the  
153 sample by inverting the tube 3-4 times and allowed it to clot under room temperature for 180  
154 minutes. Then, we spun the collected blood at 1000 × g for 15 minutes at room temperature to  
155 separate the plasma. The fluorescence intensity of FITC-d in plasma was determined with an  
156 excitation of 485 nm and an emission wavelength of 528 nm by Multimode Microplate Reader  
157 (SH-9000 serial, Corona Electric Co., Ltd., Ibaraki, Japan). The samples' fluorescence levels  
158 were converted to respective FITC-d microgram per milliliter of plasma. We made such a  
159 calculation based on a standard curve previously obtained from known levels of FITC-d.

**161 Gene expression analysis**

162 Total RNAs were extracted from ceca tissues using the RNeasy<sup>®</sup> RT Reagent (COSMO  
163 BIO Co., Ltd., Tokyo, Japan) according to the manufacturer's instructions. The concentration of  
164 RNA was quantified using a Smart Spec plus Spectrophotometer (Bio-Rad Laboratories Inc.,  
165 Tokyo, Japan). One microgram of total RNA was subjected to reverse transcription with oligo  
166 (dT<sub>18</sub>) primers using the ReverTra Ace<sup>®</sup> Master Mix kit (Toyobo CO., LTD, Osaka, Japan)  
167 according to the manufacturer's instructions. Following the QPCR Master Mix kit instructions,

1  
2  
3  
4 168 we diluted all the cDNA products 50 times with nuclear-free water and stored them at  $-20^{\circ}\text{C}$   
5  
6 169 until use.  
7  
8

9  
10 170 The quantitative real-time polymerase chain reaction (qRT-PCR) was conducted in the  
11  
12 171 Mini Opticon Real-Time PCR System (Bio-Rad Laboratories Inc.) using the Brilliant III Ultra-  
13  
14 172 Fast SYBR<sup>®</sup> Green QPCR Master Mix Kit (Agilent Technologies, West Cedar Creek, TX).  
15  
16  
17 173 Expression values were normalized to ribosomal protein S17 (RPS17) in the same sample and  
18  
19 174 then normalized to the control. The sequences of the primer pairs used for qRT-PCR  
20  
21  
22 175 amplification are listed in Table 2. Samples were heated at  $95^{\circ}\text{C}$  for 5 minutes and then  
23  
24 176 subjected to 40 cycles of denaturation at  $95^{\circ}\text{C}$  for 15 sec and annealing/elongation for 1 min at  
25  
26  
27 177  $60^{\circ}\text{C}$ . The amplifications were performed on three independent samples/groups, with triplicate  
28  
29 178 reactions carried out for each sample on the same plate. The relative mRNA level was calculated  
30  
31 179 using the  $2^{-\Delta\Delta\text{CT}}$  method (Livak & Schmittgen, 2001).  
32  
33

34 180

### 37 181 **Statistical analysis**

40 182 We represented our data as the mean  $\pm$  standard error of the mean (SEM). Data were  
41  
42 183 statistically evaluated with a one-way analysis of variance with Tukey's multiple comparison test  
43  
44  
45 184 using SPSS 20.0 software. Differences were considered significant at  $P < 0.05$  (\*) and  $P < 0.01$   
46  
47  
48 185 (\*\*).  
49  
50  
51  
52  
53  
54  
55  
56  
57  
58  
59  
60  
61  
62  
63  
64  
65

1  
2  
3  
4 186 **Results**

5  
6  
7 187 **Clinical signs and oocyst shedding**

8  
9  
10 188 Oocyst shedding started on the 6<sup>th</sup> dpi, and the maximum numbers of fecal oocysts were  
11  
12 189  $7.1 \times 10^5 \pm 4.3 \times 10^4$  oocysts/g feces on the 7<sup>th</sup> dpi (Figure 1). Diarrhea was found in all *E.*  
13  
14  
15 190 *tenella*-infected chicks from the 3<sup>rd</sup> to the 8<sup>th</sup> dpi. Diarrhea with blood was also observed from  
16  
17 191 the 4<sup>th</sup> to the 6<sup>th</sup> dpi (Table 3). In the control group, it was observed that the cecum had a smooth,  
18  
19  
20 192 glossy margin, cecum filled with feces, with no sign of bleeding or enteritis. The cecum in the  
21  
22 193 infected group showed atrophy due to dehydration, the congested serosa vessels, and the  
23  
24  
25 194 petechial bleedings were recognized while looked grossly even without opening the cecum.  
26  
27 195 Mucus and clotted blood filling the lumen of the cecum were also observed from the 4<sup>th</sup> to the 6<sup>th</sup>  
28  
29  
30 196 dpi (data not shown).

31  
32  
33 197 **Histological observations**

34  
35 198 Infiltrated cells were observed through the mucosa and submucosa from the 3<sup>rd</sup> to the 6<sup>th</sup>  
36  
37  
38 199 dpi (Figure 2; arrows). Infiltrated cells also extended through the mucosa and submucosa as well  
39  
40 200 as marked hyperplasia of epithelial cells on the 6<sup>th</sup> dpi (Figure 2D). Severe inflammation in the  
41  
42  
43 201 submucosa and the proliferation of epithelial cells of intestinal crypts were also observed on the  
44  
45 202 5<sup>th</sup> dpi and the 6<sup>th</sup> dpi (Figures 2C and D). The histopathological lesion score gradually increased  
46  
47  
48 203 from the 3<sup>rd</sup> to the 5<sup>th</sup> dpi. The maximum score was  $3.78 \pm 0.11$  on the 7<sup>th</sup> dpi (Table 3). We  
49  
50 204 observed the epithelial monolayer to be well conserved up to the 5<sup>th</sup> dpi (Figures 2A, B, and C;  
51  
52 205 arrowheads). On the other hand, a small number of epithelial layers (arrowheads) and  
53  
54  
55 206 detachment of the epithelial layer on the 6<sup>th</sup> dpi (Figure 2D). We observed **clinical signs** of  
56  
57 207 villous atrophy, severe inflammation, hemorrhage, the proliferation of epithelial cells around the  
58  
59  
60 208 intestinal crypt, and epithelial desquamation in the specimens with HE-staining cecum.

1  
2  
3  
4 209

5  
6  
7 210 **The FITC-d levels in plasma**  
8  
9

10 211 To confirm the epithelial barrier disruption caused by *E. tenella* infection, chicks were  
11  
12 212 randomly divided into three groups, administrated with FITC-d, and plasma FITC-d levels were  
13  
14  
15 213 measured as described in the Materials and Methods section. The plasma FITC-d level in *E.*  
16  
17 214 *tenella*-infected groups was significantly higher than that of the control groups during the  
18  
19  
20 215 experimental period. There was no daily increase or significant difference in the plasma FITC-d  
21  
22 216 in the fasting and control groups during the experimental period (Figures 3A and B). The plasma  
23  
24  
25 217 concentration of FITC-d in the *E. tenella* group gradually increased with the course of infection,  
26  
27 218 reaching the highest value on the 5<sup>th</sup> dpi, and it was significantly higher than the other days ( $P <$   
28  
29  
30 219  $0.05$ ; Figure 3C). The plasma FITC-d levels were  $0.292 \pm 0.013 \mu\text{g/ml}$  for the *E. tenella*-infected  
31  
32 220 group,  $0.157 \pm 0.001 \mu\text{g/ml}$  for the fasting group, and  $0.095 \pm 0.005 \mu\text{g/ml}$  for the control group  
33  
34  
35 221 on 5<sup>th</sup> dpi, especially ( $P < 0.01$ ; Figure 3D).  
36  
37

38 222

39  
40  
41 223 **The mRNA expression in *E. tenella*-infected cecum**  
42

43  
44 224 The relative mRNA expression levels of junctional molecules were determined to  
45  
46 225 evaluate the relationships between the clinical signs of *E. tenella* infection and its increasing  
47  
48  
49 226 permeability. Relative mRNA expression levels of CLDN-1 showed a significant decrease at 4<sup>th</sup>  
50  
51 227 dpi but were sharply raised on the 5<sup>th</sup> and 6<sup>th</sup> dpi compared with the control. CLDN-2 were  
52  
53 228 significantly increased on the 3<sup>rd</sup>, 4<sup>th</sup>, and 5<sup>th</sup> dpi compared with the control group (Figures 4).  
54  
55  
56 229 On the other hand, the mRNA expression levels of CLDN-3, OCDN, and ZO-1 tended to  
57  
58 230 decrease throughout the experimental period compared with the control group (Figures 4 and 5).  
59  
60  
61  
62  
63  
64  
65

1  
2  
3  
4  
5  
6  
7  
8  
9  
10  
11  
12  
13  
14  
15  
16  
17  
18  
19  
20  
21  
22  
23  
24  
25  
26  
27  
28  
29  
30  
31  
32  
33  
34  
35  
36  
37  
38  
39  
40  
41  
42  
43  
44  
45  
46  
47  
48  
49  
50  
51  
52  
53  
54  
55  
56  
57  
58  
59  
60  
61  
62  
63  
64  
65

231 The OCDN expression levels were significantly reduced on the 4<sup>th</sup> and 5<sup>th</sup> dpi compared with the  
232 uninfected control group (Figure 5). As shown in Figure 5, the relative expression level of ZO-1  
233 mRNA was especially reduced on the 5<sup>th</sup> and 6<sup>th</sup> dpi in cecum compared with uninfected control  
234 ( $P < 0.05$ ). The E-cadherin (E-cad) gene expression was significantly lower during the  
235 experimental period. The JAM-2 expression levels in the cecum showed no significant difference  
236 during the experimental period.

237 We also measured mRNA expression levels of pro-inflammatory cytokines such as  
238 interleukin (IL)-1 $\beta$ , IL-17A, IL-22, interferon (IFN)- $\gamma$ , and tumor necrosis factor (TNF)- $\alpha$   
239 (Figure 6). The expression levels of IFN- $\gamma$  tended to increase with the course of infection, but no  
240 statistical significance was observed. The expressions of IL-1 $\beta$  and IL-22 were significantly  
241 increased on the 4<sup>th</sup> to the 6<sup>th</sup> dpi in the *E. tenella*-infected chicks compared to control. The  
242 mRNA expression level of IL-17A in infected chicks was considerably higher than normal  
243 chicks at 2<sup>nd</sup> dpi. There was no significant difference in gene expression of TNF- $\alpha$ .

## 244 Discussion

245 This study investigates the association between the expression pattern of intestinal  
246 epithelial barrier molecules and typical clinical signs in chicks with *E. tenella*. The infection of  
247 *E. tenella* is typically accompanied by severe diarrhea and bloody feces, with blood retention in  
248 the cecum (Chapman, 2014; El-Ashram et al., 2019). In this study, *E. tenella* infected chicks  
249 indicated diarrhea from 3<sup>rd</sup> to 8<sup>th</sup> dpi and bloody feces from 4<sup>th</sup> to 6<sup>th</sup> dpi as clinical signs. Similar  
250 research has reported that chicks with *E. tenella* infection had reported the emergence of bloody  
251 diarrhea from 4<sup>th</sup> to 7<sup>th</sup> dpi (Lan et al., 2016). This difference in duration of clinical signs may be  
252 due to differences in the virulence of parasite strain and the number of oocysts used because the  
253 number of oocysts in their study was about 2.5 times compared to our study. Regarding  
254 histological observations of cecum specimens, our results show that the epithelial monolayer was  
255 well maintained at 3<sup>rd</sup> and 4<sup>th</sup> dpi. On the other hand, the lesion score, which corresponds to cecal  
256 damages, has been significantly increased from 4<sup>th</sup> dpi, reaching the maximum at 5<sup>th</sup> dpi until 8<sup>th</sup>  
257 dpi. Histopathological observations in our study indicated the loss of cecal villi, necrosis, and  
258 hemorrhage at 6<sup>th</sup> dpi on cecal mucosa, which is similar to previous reports (Sharma et al., 2015;  
259 Abdelrazek et al., 2020). Oocyst shedding started from the 6<sup>th</sup> dpi onwards, in agreement with  
260 other studies (Zhou et al., 2020; Jordan et al., 2011). Some researchers attributed clinical signs of  
261 *Eimeria* infection to damages in blood vessels due to the release of merozoite from second-  
262 generation schizonts (Burrell et al., 2019; Fernando et al., 1983; Macdonald et al., 2017). Lopez  
263 et al. (2020) have reported that the first and second generations of schizonts release merozoites at  
264 3<sup>rd</sup> to 5<sup>th</sup> dpi and the oocyst shedding occurs at 6<sup>th</sup> dpi onwards. Especially, second-generation  
265 schizonts are large and develop deeply in the lamina propria. Therefore, once merozoites are  
266 released, blood vessels are disrupted (McKenzie et al., 1985), explaining the presence of blood in

1  
2  
3  
4  
5  
6  
7  
8  
9  
10  
11  
12  
13  
14  
15  
16  
17  
18  
19  
20  
21  
22  
23  
24  
25  
26  
27  
28  
29  
30  
31  
32  
33  
34  
35  
36  
37  
38  
39  
40  
41  
42  
43  
44  
45  
46  
47  
48  
49  
50  
51  
52  
53  
54  
55  
56  
57  
58  
59  
60  
61  
62  
63  
64  
65

feces at 4<sup>th</sup> dpi and the increases of lesion scores at 4<sup>th</sup> and 5<sup>th</sup> dpi. Findings in this study also indicates that the timing of clinical signs such as bloody feces occurred at a time that corresponds to the life cycle of *Eimeria* spp. in chickens. Hence, our results may suggest that diarrhea and bloody feces at the early stage of *E. tenella* infection are related to the destruction of intraepithelial cell junctions rather than the detachment of the epithelial layer.

To evaluate the intestinal permeability associated with the disruption of the epithelial barrier in the cecum with *E. tenella*, the levels of FITC-d in plasma of each experimental group were determined. As shown in Figure 3, the concentrations of FITC-d in both fasting and *E. tenella*-infected groups were much higher than the control group from the 2<sup>nd</sup> to 6<sup>th</sup> dpi. Although no change was observed in FITC-d plasma levels in both fasting and the control groups between the days, plasma FITC-d levels in *E. tenella*-infected group increased with the course of infection, peaking on the 5<sup>th</sup> dpi. Teng et al (2020) have reported gastrointestinal leakage in chickens with *Eimeria* infection was rapidly elevated at 5<sup>th</sup> dpi. Results in this study are similar to Teng et al. Further to that, results show that a significant increase of lesion score after 4<sup>th</sup> dpi was tightly associated with high plasma levels of FITC-d at 4<sup>th</sup> to 6<sup>th</sup> dpi, with rapid progression of epithelial barrier leakage during this period. These results indicate that cecal permeability increases in the *E. tenella* infection early stage, suggesting that the epithelial barrier condition was affected as the parasite life cycle progressed.

The relations between clinical signs of *Eimeria* infection, the status of the intestinal immunity, and the epithelial barrier at the small intestine have been reported in some previous studies (Hong et al., 2006; Park et al., 2020; Teng et al., 2020). However, molecular insights associated with clinical signs of *E. tenella* infection at the cecum have not been well evaluated in the past. Tight junction proteins are adhesive junctional molecules that link epithelial cells



1  
2  
3  
4  
5  
6  
7  
8  
9  
10  
11  
12  
13  
14  
15  
16  
17  
18  
19  
20  
21  
22  
23  
24  
25  
26  
27  
28  
29  
30  
31  
32  
33  
34  
35  
36  
37  
38  
39  
40  
41  
42  
43  
44  
45  
46  
47  
48  
49  
50  
51  
52  
53  
54  
55  
56  
57  
58  
59  
60  
61  
62  
63  
64  
65

290 together and regulate epithelial barrier function, permitting the passive entry of nutrients, ions,  
291 and water, while blocking the entrance of pathogen access to underlying tissue compartments.  
292 (Groschwitz et al., 2009). Awad et al. (2017) have studied enteric pathogens and their toxin-  
293 induced disruption of the intestinal barrier by altering tight junctions in chickens. The CLDNs  
294 are the main components of tight junctions and form a seal that modulates paracellular transport  
295 in the intestinal epithelium. The CLDNs exist in two different classes, sealing claudins and pore-  
296 forming claudins (Itallie & Anderson, 2006). It is known that CLDN-1 and -3 are sealing  
297 claudins, of which increased expression leads to a tight epithelium (Haworth et al., 2005; Milatz  
298 et al., 2010). In contrast, CLDN-2 is considered as the pore-forming claudin. It creates  
299 paracellular anion/cation pores and water channels that decrease the epithelial tightness and  
300 increase the solute permeability by allowing the passage of sodium ions (France & Turner, 2017;  
301 Furuse et al., 2001). The result in Figure 4 indicated that CLDN-1 mRNA level was first  
302 decreased at 4<sup>th</sup> dpi ( $P < 0.05$ ), but later remarkably increased at 5<sup>th</sup> and 6<sup>th</sup> dpi ( $P < 0.05$ ). Teng  
303 et al. (2020) have reported that CLDN-1 gene expression increases at 6<sup>th</sup> dpi in the small  
304 intestine of chicks with the *Eimeria* challenge. As CLDN-1 plays an important role in  
305 maintaining intestinal barrier integrity, the higher expression of CLDN-1 helps the chick to  
306 retrieve intestinal integrity. This could be related to the acute mechanisms of repair in the injured  
307 intestinal epithelium (Slifer & Blikslager, 2020).

The expression of CLDN-2 was significantly higher at 3<sup>rd</sup>, 4<sup>th</sup>, and 5<sup>th</sup> dpi (Figure 4).

309 Higher expressions of pore-forming proteins facilitate the paracellular permeability by allowing  
310 more luminal contents to translocate to the systemic circulation (Wada et al., 2013). Researchers  
311 reported that increased CLDN-2 is associated with barrier disruption in response to inflammation

1  
2  
3  
4  
5  
6  
7  
8  
9  
10  
11  
12  
13  
14  
15  
16  
17  
18  
19  
20  
21  
22  
23  
24  
25  
26  
27  
28  
29  
30  
31  
32  
33  
34  
35  
36  
37  
38  
39  
40  
41  
42  
43  
44  
45  
46  
47  
48  
49  
50  
51  
52  
53  
54  
55  
56  
57  
58  
59  
60  
61  
62  
63  
64  
65

312 and infection (Ahmad et al., 2014; Furuse et al., 2001). This study, finds that the upregulation of  
313 CLDN-2 gene expression could induce diarrhea by draining water into the cecal lumen.

314 The results in this study also indicated that the CLDN-3 expression levels tended to be  
315 low during the experimental period compared with the control group, especially on the 3<sup>rd</sup> and  
316 the 6<sup>th</sup> dpi (Figure 4). These results might suggest that the reduction of CLDN-3 was part of the  
317 increased paracellular permeability, resulting in the leakage of blood and other substances  
318 through this route. Several researchers also reported a decrease of sealing proteins, resulting in a  
319 leak epithelial barrier and harmful movement of luminal contents through the paracellular space  
320 (Haworth et al., 2005; Milatz et al., 2010).

321 The role of OCDN is to maintain the tight junction barrier and regulate paracellular pore  
322 and leak pathways (France & Turner, 2017; Itallie et al. 2010; Hossain & Hirata, 2008). Cani et  
323 al. (2009) claimed that the expression of OCDN was decreased and contrariwise correlated with  
324 the FITC-d's translocation from the intestinal tract to the bloodstream, associated with the  
325 presence of diarrhea, highlighting the importance of OCDN in maintaining the barrier function.

326 Chen et al. (2015) has reported that the *Eimeria* parasite challenge induces gut barrier failure and  
327 inflammation in broilers by the upregulation of certain cytokines and the downregulation of  
328 OCDN in jejunum mucosa, and elevated levels of endotoxin and acid glycoprotein in their  
329 serum. In this study, the OCDN expression level tended to reduce during the experimental period  
330 and significantly decreased at 4<sup>th</sup> and 5<sup>th</sup> dpi. ZO-1 proteins help cell-cell contacts and were  
331 enriched at cell junctions in epithelial cells (Furuse et al., 2001). In this study, the expression  
332 level of ZO-1 decreased after the 3<sup>rd</sup> dpi and reduced considerably on the 5<sup>th</sup> and the 6<sup>th</sup> dpi.  
333 These findings were consistent with a previous report, suggesting that the gene expression of  
334 ZO-1 is reduced as a consequence of parasite infection (Teng et al., 2021).

1  
2  
3  
4 335 According to Lechuga & Ivanov (2017), E-cad proteins are critical molecules of the  
5  
6 336 adherens junction. Intestinal epithelial cells predominantly express E-cad. In this study, the  
7  
8  
9 337 expression level of E-cad was significantly reduced during the experimental period. Similarly,  
10  
11  
12 338 previous studies indicates that the infections of *E. vermiformis* (Inagaki et al., 2006) and  
13  
14 339 *Cryptosporidium parvum* consequently resulted in the downward tendency of E-cad expression  
15  
16 340 (Kumar et al., 2018). This data suggested that the early downregulation of E-cad gene expression  
17  
18  
19 341 could contribute to the barrier dysfunction and increased permeability in the onset of *E. tenella*  
20  
21 342 infection.

22  
23  
24 343 The tight junction proteins can be regulated by many factors including cytokines and  
25  
26 344 growth factors (Petcchia et al., 2012). In the previous research, IL-17A's neutralization  
27  
28  
29 345 increased tissue damages in the dextran-sulfate-induced acute colitis model (Ogawa et al., 2004).  
30  
31  
32 346 This suggests that IL-17A has an essential function in maintaining the barrier function of the  
33  
34 347 intestinal epithelial barrier. Lee et al. (2015) added that the absence of IL-17A increased the  
35  
36 348 epithelial injury and compromised the acute colitis model's barrier function. In this study, the  
37  
38  
39 349 expression of IL-17A was suppressed at 3<sup>rd</sup> dpi onwards which coincided with the reduction of  
40  
41 350 several junctional gene expressions (Figures 5 and 6). This implies that the decreased level of IL-  
42  
43  
44 351 17A might suppress the expression of related junctional genes, including ZO-1, and therefore  
45  
46 352 disrupt the barrier function in the cecum. Furthermore, IL-17A can induce the expression of pro-  
47  
48  
49 353 inflammatory cytokines such as IL-1 $\beta$  and IL-6 from epithelial cells and fibroblasts (Iwakura et  
50  
51 354 al., 2011; Gaffen et al., 2009). In this study, the upregulations of IL-1 $\beta$  and IL-22 gene  
52  
53  
54 355 expressions had become significant from 4<sup>th</sup> dpi going forward, which was after the high  
55  
56 356 expression of IL-17A at 2<sup>nd</sup> dpi. This indicates that the transient expression of IL-17A at the  
57  
58  
59 357 early stage of *E. tenella* infection has triggered the latter expression of IL-1 $\beta$  and IL-22.  
60  
61  
62  
63  
64  
65

1  
2  
3  
4  
5  
6  
7  
8  
9  
10  
11  
12  
13  
14  
15  
16  
17  
18  
19  
20  
21  
22  
23  
24  
25  
26  
27  
28  
29  
30  
31  
32  
33  
34  
35  
36  
37  
38  
39  
40  
41  
42  
43  
44  
45  
46  
47  
48  
49  
50  
51  
52  
53  
54  
55  
56  
57  
58  
59  
60  
61  
62  
63  
64  
65

358 Previous studies have mentioned the roles of IL-22 in protecting and regenerating cells in  
359 the gastrointestinal tract (Eyerich et al., 2017). Besides, IL-22 is also important in innate  
360 immunity and epithelial reorganization (Wolk et al., 2006). This study indicates that higher  
361 expressions of IL-22 in *E. tenella* infected chicks had been observed from the 4<sup>th</sup> to the 6<sup>th</sup> dpi.  
362 Under the inflammation process, tissues including the intestinal epithelium are exposed to  
363 multiple cytokines (Hong et al., 2006). Among those, IL-1 $\beta$  is an inflammatory cytokine with  
364 diverse physiological functions and pathological significances, which plays an important role in  
365 health and disease and is often increased in the impaired intestine (Kaneko et al., 2019). It was  
366 reported that the IL-1 $\beta$  mRNA level was highly upregulated after parasite and bacterial  
367 infections (Laurent et al., 2001; Withanage et al., 2004). Moreover, a recent study utilizing a  
368 chicken macrophage microarray also identified that the IL-1 $\beta$  transcripts were elevated during  
369 experimental coccidiosis (Dalloul et al., 2007). A direct correlation was found in the mRNA  
370 expression levels between OGDN and IL-1 $\beta$  in this study. Therefore, it may be concluded that  
371 IL-1 $\beta$  impairs the intestinal tight junction barrier by decreasing OGDN expression.

372 IFN- $\gamma$  is known to play as a mediator that enhances epithelial permeability via the  
373 disruption of tight junction complexes (Willemsen et al., 2005). Ferrier et al. (2003) has reported  
374 the relationship between stress-induced intestinal permeability and increased mucosal IFN- $\gamma$   
375 expression. Willemsen et al. (2005) has reported that the induction of CLDN-2 by IFN- $\gamma$  is one  
376 of the etiological factors of intestinal barrier dysfunction. In our experiment, the IFN- $\gamma$   
377 expression in infected chickens seems to be higher than that compared to the control from 3<sup>rd</sup> to  
378 6<sup>th</sup> dpi, although this difference was not significant (Figure 6). Previous research has also  
379 reported that TNF- $\alpha$  plays an important role in the proinflammatory cytokines-induced intestinal  
380 barrier disruption (Ma et al., 2004; Graham et al., 2006; Ye et al., 2008). However, in this study,

1  
2  
3  
4  
5  
6  
7  
8  
9  
10  
11  
12  
13  
14  
15  
16  
17  
18  
19  
20  
21  
22  
23  
24  
25  
26  
27  
28  
29  
30  
31  
32  
33  
34  
35  
36  
37  
38  
39  
40  
41  
42  
43  
44  
45  
46  
47  
48  
49  
50  
51  
52  
53  
54  
55  
56  
57  
58  
59  
60  
61  
62  
63  
64  
65

381 TNF- $\alpha$  was also no significant difference between control and infected chickens. It is not known  
382 whether this derives from the diverse attack mechanisms of the parasite itself or the result of the  
383 host mechanism to rebalance the barrier function experiments are needed to further explore this  
384 matter.

385 In conclusion, this is the first study to describe daily changes in intestinal junctional gene  
386 expressions upon *E. tenella* infection in chick cecum. The findings in this study, suggest that the  
387 expression of junctional molecule genes are related to clinical signs such as diarrhea and bloody  
388 feces in chicks infected with *E. tenella*. The disruption of barrier function via downregulation of  
389 CLDN-1, CLDN-3, E-cad, OCDN, and ZO-1, but increased CLDN-2, could contribute to *E.*  
390 *tenella* infection-induced diarrhea. Furthermore, this study, reports a link between the high levels  
391 of pro-inflammatory cytokines and junctional molecules related to the epithelial barrier and  
392 intestinal permeability. Insights on the inflammation-dependent alterations of junctional gene  
393 expressions will provide new ideas in the development of therapeutics for improving mucosal  
394 healing and barrier function in *E. tenella* infection. Further *in vitro* studies will be needed to  
395 verify the relationship between *E. tenella*-induced alteration of apical junctional complexes  
396 proteins and responses of host epithelial cells and their impacts on barrier function.

397

1  
2  
3  
4  
5  
6  
7  
8  
9  
10  
11  
12  
13  
14  
15  
16  
17  
18  
19  
20  
21  
22  
23  
24  
25  
26  
27  
28  
29  
30  
31  
32  
33  
34  
35  
36  
37  
38  
39  
40  
41  
42  
43  
44  
45  
46  
47  
48  
49  
50  
51  
52  
53  
54  
55  
56  
57  
58  
59  
60  
61  
62  
63  
64  
65

398 **Declaration of Competing Interest**

399 The authors declare no competing financial conflicts of interest.

400

401 **Funding**

402 This work was supported by the Research Grant for Encouragement of Students from the  
403 Graduate school of Environmental and Life Science, Okayama University.

404

405 **Acknowledgments**

406 We would like to thank Dr. Dung Thi Ho at Hue University of Agriculture and Forestry and Mr.  
407 Kazuma Toda at Okayama University for their help. We also thank Dr. Yuki Yamamoto, Dr.  
408 Koji Kimura, and their colleagues at Okayama University for their technical equipment  
409 assistance. The authors would like to thank **Mr. Kondwani Chiumya and** Enago ([www.enago.jp](http://www.enago.jp))  
410 for the English language review.

1  
2  
3  
4  
5  
6  
7  
8  
9  
10  
11  
12  
13  
14  
15  
16  
17  
18  
19  
20  
21  
22  
23  
24  
25  
26  
27  
28  
29  
30  
31  
32  
33  
34  
35  
36  
37  
38  
39  
40  
41  
42  
43  
44  
45  
46  
47  
48  
49  
50  
51  
52  
53  
54  
55  
56  
57  
58  
59  
60  
61  
62  
63  
64  
65

411 **References**

412 Abdelrazek, Y., Desouky, M., Khaled, Sultan., Nagwa, M., Elhawary, Ammar, N., 2020.  
413 Levamisole Hydrochloride as Immunostimulant Drug Synergies the Effect of Eimeria  
414 tenella Lab- made Vaccine Experimental Trial. Asian J of Animal Sciences. 14, 54-60.

415 Ahmad, R., Chaturvedi, R., Olivares-Villagómez, D., Habib, T., Asim, M., Shivesh, P., Polk, D.  
416 B., Wilson, K. T., Washington, M. K., Kaer, L. van, Dhawan, P., & Singh, A. B., 2014.  
417 Targeted colonic claudin-2 expression renders resistance to epithelial injury, induces  
418 immune suppression, and protects from colitis. Mucosal Immunology, 7, 1340–1353.

419 Awad, W. A., Hess, C., & Hess, M., 2017. Enteric pathogens and their toxin-induced disruption  
420 of the intestinal barrier through alteration of tight junctions in chickens. Toxins, 9.

421 Burrell, A., Tomley, F. M., Vaughan, S., & Hernandez, V., 2019. Life cycle stages, specific  
422 organelles, and invasion mechanisms of Eimeria species. Parasitology, 147, 263-278.

423 Cani, P. D., Possemiers, S., van de Wiele, T., Guiot, Y., Everard, A., Rottier, O., Geurts, L.,  
424 Naslain, D., Neyrinck, A., Lambert, D. M., Muccioli, G. G., & Delzenne, N. M., 2009.  
425 Changes in gut microbiota control inflammation in obese mice through a mechanism  
426 involving GLP-2-driven improvement of gut permeability. Gut, 58, 1091–1103.

427 Chapman, H. D., 2014. Milestones in avian coccidiosis research: A review. Poultry Science, 93,  
428 501–511.

429 Chen, J., Tellez, G., Richards, J.D., & Escobar, J., 2015. Identification of potential biomarkers  
430 for gut barrier failure in broiler chickens. Front. Vet. Sci, 2,14.

431 Chelakkot, C., Ghim, J., & Ryu, S. H., 2018. Mechanisms regulating intestinal barrier integrity  
432 and its pathological implications. Experimental and Molecular Medicine, 50.

1  
2  
3  
4 433 Chida, R. U., An, J. H., & Soda, H. I., 2009. Effect of Capsaicin on the Tight Junctional  
5  
6 434 Permeability of the Human Intestinal Cells. *Journal of Arid Land Studies*, 19, 89–92.  
7  
8  
9 435 Chow, Y. P., Wan, K. L., Blake, D. P., Tomley, F., & Nathan, S., 2011. Immunogenic *Eimeria*  
10  
11 436 *tenella* glycosylphosphatidylinositol-anchored surface antigens (SAGs) induce  
12  
13  
14 437 inflammatory responses in avian macrophages. *PLoS ONE*, 6.  
15  
16 438 Dalloul, R. A., & Lillehoj, H. S., 2006. Poultry coccidiosis: recent advancements in control  
17  
18  
19 439 measures and vaccine development. *Expert Review of Vaccines*, 5, 143–163.  
20  
21 440 Dalloul, R. A., Bliss, T. W., Hong, Y.-H., Ben-Chouikha, I., Park, D. W., Keeler, C. L., &  
22  
23 441 Lillehoj, H. S., 2007. Unique responses of the avian macrophage to different species of  
24  
25  
26 442 *Eimeria*. *Molecular Immunology*, 44, 558–566.  
27  
28  
29 443 El-Ashram, S., Aboelhadid, S. M., Arafa, W. M., Gadelhaq, S. M., & Abdel-Razik, A. R. H.,  
30  
31 444 2019. Protective potential of diclazuril-treated oocysts against coccidiosis in layer chicks.  
32  
33 445 *Veterinary Parasitology*, 273, 105–111.  
34  
35  
36 446 Erben, U., Loddenkemper, C., Doerfel, K., Spieckermann, S., Haller, D., Heimesaat, M. M.,  
37  
38 447 Zeitz, M., Siegmund, B., & Kühl, A. A., 2014. A guide to histomorphological evaluation of  
39  
40  
41 448 intestinal inflammation in mouse models. *Int J Clin Exp Pathol*, 7, 4557–4576.  
42  
43 449 Estela Quiroz-Castaneda, R., & Dantan-Gonzalez, E., 2015. Control of Avian Coccidiosis:  
44  
45 450 Future and Present Natural Alternatives. *BioMed Research International*, 2015, 1–11.  
46  
47  
48 451 Eyerich, K., Dimartino, V., & Cavani, A., 2017. IL-17 and IL-22 in immunity: Driving  
49  
50 452 protection and pathology. *European Journal of Immunology*, 47, 607–614.  
51  
52  
53 453 Fernando, M. A. A., Rose, M. E., & Al-Attar, M. A., 1983. Invasion of Chicken Caecal and  
54  
55 454 Intestinal Lamina Propria by Crypt Epithelial cells Infected with *Coccidia*. *Parasitology*, 86,  
56  
57  
58 455 391–398.  
59  
60  
61  
62  
63  
64  
65



1  
2  
3  
4  
5  
6  
7  
8  
9  
10  
11  
12  
13  
14  
15  
16  
17  
18  
19  
20  
21  
22  
23  
24  
25  
26  
27  
28  
29  
30  
31  
32  
33  
34  
35  
36  
37  
38  
39  
40  
41  
42  
43  
44  
45  
46  
47  
48  
49  
50  
51  
52  
53  
54  
55  
56  
57  
58  
59  
60  
61  
62  
63  
64  
65

456 Ferrier, L., Mazelin, L., Cenac, N., Desreumaux, P., Janin, A., Emilie, D., Colombel, J.F.,

457 Garcia-Villar, R., Fioramonti, J., & Bueno, L., 2003. Stress-induced disruption of colonic

458 epithelial barrier: role of interferon-gamma and myosin light chain kinase in mice.

459 *Gastroenterology Sep*, 125, 795-804.

460 France, M. M., & Turner, J. R., 2017. The mucosal barrier at a glance. *Journal of Cell Science*,  
461 130, 307–314.

462 Furuse, M., Furuse, K., Sasaki, H., & Tsukita, S., 2001. Conversion of Zonulae Occludentes  
463 from Tight to Leaky Strand Type by Introducing Claudin-2 into Madin-Darby Canine  
464 Kidney I Cells. *The Journal of Cell Biology*, 153, 263–272.

465 Gaffen, S. L., 2009. Structure and signaling in the IL-17 receptor family. *Nature Review of*  
466 *Immunology*, 9, 556–567.

467 Graham, W. V., Wang, F., Clayburgh, D. R., Cheng, J. X., Yoon, B., 2006. Tumor necrosis

468 factor-induced long myosin light chain kinase transcription is regulated by differentiation-

469 dependent signaling events. characterization of the human long myosin light chain kinase

470 promoter. *J Biol Chem*, 281, 26205–26215.

471 Groschwitz, K. R., & Hogan, S. P., 2009. Intestinal Barrier Function: Molecular Regulation and  
472 Disease Pathogenesis. *J Allergy Clin Immunol*, 124, 3–22.

473 Gyorke, A., Pop, L., & Cozma, V., 2013. Prevalence and distribution of Eimeria species in  
474 broiler chicken farms of different capacities. *Parasite*, 20.

475 Haworth, K. E., El-Hanfy, A., Prayag, S., Healy, C., Dietrich, S., & Sharpe, P., 2005. Expression  
476 of Claudin-3 during chick development. *Gene Expression Patterns*, 6, 40–44.

1  
2  
3  
4  
5  
6  
7  
8  
9  
10  
11  
12  
13  
14  
15  
16  
17  
18  
19  
20  
21  
22  
23  
24  
25  
26  
27  
28  
29  
30  
31  
32  
33  
34  
35  
36  
37  
38  
39  
40  
41  
42  
43  
44  
45  
46  
47  
48  
49  
50  
51  
52  
53  
54  
55  
56  
57  
58  
59  
60  
61  
62  
63  
64  
65

477 Ho, T. D., Pham, H. S. H., Aota, W., Matsubayashi, M., Tsuji, N., Hatabu, T., 2021. Reduction  
478 of macrophages by carrageenan decreases oocyst output and modifies local immune  
479 reaction in chick cecum with *Eimeria tenella*. *Research in Veterinary Science*, 139, 59-66.

480 Hong, Y. H., Lillehoj, H. S., Lee, S. H., Dalloul, R. A., & Lillehoj, E. P., 2006. Analysis of  
481 chicken cytokine and chemokine gene expression following *Eimeria acervulina* and  
482 *Eimeria tenella* infections. *Veterinary Immunology and Immunopathology*, 114, 209–223.

483 Hossain, Z., & Hirata, T., 2008. Molecular mechanism of intestinal permeability: interaction at  
484 tight junctions. *Molecular BioSystems*, 4, 1181–1185.

485 Ikenouchi, J., Umeda, K., Tsukita, S., Furuse, M., & Tsukita, S., 2007. Requirement of ZO-1 for  
486 the formation of belt-like adherens junctions during epithelial cell polarization. *Journal of*  
487 *Cell Biology*, 176, 779–786.

488 Inagaki-Ohara, K., Dewi, F. N., Hisaeda, H., Smith, A. L., Jimi, F., Miyahira, M., Abdel, A.,  
489 Horii, Y., & Nawa, Y., 2006. Intestinal intraepithelial lymphocytes sustain the epithelial  
490 barrier function against *E. vermiformis* infection. *Infection and Immunity*, 74, 5292–5301.

491 Jordan, D. J., Caldwell, J., Klein, J., Coppedge, S., Pohl, S., Fitz-Coy, & Lee, J. T., 2011.  
492 *Eimeria tenella* oocyst shedding and output in cecal or fecal contents following  
493 experimental challenge in broilers. *Poultry Science*, 90, 990–995.

494 Iwakura, Y., Ishigame, H., Saijo, S., & Nakase, S., 2011. Functional specialization of  
495 interleukin-17 family members. *Immunity*, 34, 149–162.

496 Kaneko, N., Kurata, M., Yamamoto, T., Morikawa, S., & Masumoto, J., 2019. The role of  
497 interleukin-1 in general pathology. *Inflammation and Regeneration*, 39, 1–16.

498 Kumar, A., Chatterjee, I., Anbazhagan, A. N., Jayawardena, D., Priyamvada, S., Alrefai, W. A.,  
499 Sun, J., Borthakur, A., & Dudeja, P. K., 2018. *Cryptosporidium parvum* disrupts intestinal

1  
2  
3  
4  
5  
6  
7  
8  
9  
10  
11  
12  
13  
14  
15  
16  
17  
18  
19  
20  
21  
22  
23  
24  
25  
26  
27  
28  
29  
30  
31  
32  
33  
34  
35  
36  
37  
38  
39  
40  
41  
42  
43  
44  
45  
46  
47  
48  
49  
50  
51  
52  
53  
54  
55  
56  
57  
58  
59  
60  
61  
62  
63  
64  
65

500 epithelial barrier function via altering expression of key tight junction and adherens junction  
501 proteins. Cellular Microbiology, 20, 1–13.

502 Kuttappan, V. A., Vicuna, E. A., Latorre, J. D., Wolfenden, A. D., Téllez, G. I., Hargis, B. M., &  
503 Bielke, L. R., 2015. Evaluation of gastrointestinal leakage in multiple enteric inflammation  
504 models in chickens. Frontiers in Veterinary Science, 2.

505 Lan, L., Zuo, B., Ding, H., Huang, Y., Chen, X., Du, A., 2016. Anticoccidial evaluation of a  
506 traditional Chinese medicine *Brucea javanica* in broilers, Poultry Science, 95, 811-818.

507 Laurent, F., Mancassola, R., Lacroix, S., Menezes, R., & Naciri, M., 2001. Analysis of Chicken  
508 Mucosal Immune Response to *Eimeria tenella* and *Eimeria maxima* Infection by  
509 Quantitative Reverse Transcription-PCR. Infection and Immunity, 69, 2527–2534.

510 Lechuga, S., & Ivanov, A. I., 2017. Disruption of the epithelial barrier during intestinal  
511 inflammation: Quest for new molecules and mechanisms. Biochimica et Biophysica Acta -  
512 Molecular Cell Research, 1864, 1183–1194.

513 Lee, J. S., Tato, C. M., Joyce, B., Gulen, M. F., Cayatte, C., Chen, Y., Blumenschein, W., Judo,  
514 M., Ayanoglu, G., McClanahan, T., Li, X. & Cua, D. J., 2015. Interleukin-23-independent  
515 IL-17 production regulates intestinal epithelial permeability. Immunity, 43, 727–738.

516 Livak, K. J., & Schmittgen, T. D., 2001. Analysis of relative gene expression data using real-  
517 time quantitative PCR and the  $2^{-\Delta\Delta CT}$  method. Methods, 25, 402–408.

518 Lopez-Osorio, S., Chaparro-Gutierrez. J. J., Gomez-Osorio, L. M., 2020. Overview of Poultry  
519 *Eimeria* Life Cycle and Host-Parasite Interactions. Front Vet Sci, 7, 384.

520 Ma, T. Y., Iwamoto, G. K., Hoa, N. T., Akotia, V., Pedram, A., 2004. TNF- $\alpha$ -induced increase in  
521 intestinal epithelial tight junction permeability requires NF- $\kappa$ B activation. Am J Physiol  
522 Gastrointest Liver Physiol, 286, G367–G376.

1  
2  
3  
4 523 Macdonald, S. E., Nolan, M. J., Harman, K., Boulton, K., Hume, D. A., Tomley, F. M., Stabler,  
5  
6  
7 524 R. A., & Blake, D. P., 2017. Effects of *E. tenella* infection on chicken caecal microbiome  
8  
9 525 diversity, exploring variation associated with severity of pathology, PLoS ONE, 12.  
10  
11 526 McKenzie, M. E., Johnson, J., Long, P. L., 1985. Lethality of intestinal tissue extracts from  
12  
13  
14 527 *Eimeria*-infected. *Parasitology*, 90, 565-572.  
15  
16 528 Milatz, S., Krug, S. M., Rosenthal, R., Günzel, D., Müller, D., Schulzke, J.-D., Amasheh, S., &  
17  
18  
19 529 Fromm, M., 2010. Claudin-3 acts as a sealing component of the tight junction for ions of  
20  
21 530 either charge and uncharged solutes. *Biochimica et Biophysica Acta (BBA) -*  
22  
23  
24 531 *Biomembranes*, 1798.  
25  
26 532 Odenwald, M. A., & Turner, J. R., 2017. The intestinal epithelial barrier: A therapeutic target?  
27  
28  
29 533 *Nature Reviews Gastroenterology and Hepatology*, 14, 9–21.  
30  
31 534 Ogawa, A., Andoh, A., Araki, Y., Bamba, T., & Fujiyama, Y., 2004. Neutralization of  
32  
33  
34 535 interleukin-17 aggravates dextran sulfate sodium-induced colitis in mice. *Clinical*  
35  
36 536 *Immunology*, 110, 55–62.  
37  
38 537 Park, I., Lee, Y., Goo, D., Zimmerman, N. P., Smith, A. H., Rehberger, T., & Lillehoj, H. S.,  
39  
40  
41 538 2020. The effects of dietary *Bacillus subtilis* supplementation, as an alternative to  
42  
43 539 antibiotics, on growth performance, intestinal immunity, and epithelial barrier integrity in  
44  
45  
46 540 broiler chickens infected with *Eimeria maxima*. *Poultry Science*, 99, 725–733.  
47  
48 541 Petecchia, L., Sabatini, F., Usai, C., Caci, E., Varesio, L., & Rossi, G. A., 2012. Cytokines  
49  
50  
51 542 induce tight junction disassembly in airway cells via an EGFR-dependent MAPK/ERK1/2-  
52  
53 543 pathway. *Laboratory Investigation*, 92, 1140–1148.  
54  
55 544 Reid, A. J., Blake, D. P., Ansari, H. R., Billington, K., Browne, H. P., Bryant, J., Dunn, M.,  
56  
57  
58 545 Hung, S. S., Kawahara, F., Miranda-Saavedra, D., Malas, T. B., Mourier, T., Naghra, H.,  
59  
60  
61  
62  
63  
64  
65

1  
2  
3  
4  
5  
6  
7  
8  
9  
10  
11  
12  
13  
14  
15  
16  
17  
18  
19  
20  
21  
22  
23  
24  
25  
26  
27  
28  
29  
30  
31  
32  
33  
34  
35  
36  
37  
38  
39  
40  
41  
42  
43  
44  
45  
46  
47  
48  
49  
50  
51  
52  
53  
54  
55  
56  
57  
58  
59  
60  
61  
62  
63  
64  
65

546 Nair, M., Otto, T. D., Rawlings, N. D., Rivailler, P., Sanchez-Flores, A., Sanders, M., Pain,  
547 A., 2014. Genomic analysis of the causative agents of coccidiosis in domestic chickens.  
548 *Genome Research*, 24, 1676–1685.

549 Ritzi, M. M., Abdelrahman, W., Van-Heerden, K., Mohnl, M., Barrett, N. W., & Dalloul, R. A.,  
550 2016. Combination of probiotics and coccidiosis vaccine enhances protection against an  
551 *Eimeria* challenge. *Veterinary Research*, 47, 1–8.

552 Sharma, S., Azmi, S., Iqbal, A., Nasirudullah, N., Mushtaq, I., 2015. Pathomorphological  
553 alterations associated with chicken coccidiosis in Jammu division of India. *Journal of*  
554 *Parasitic Diseases*. 39, 147-151.

555 Slifer, Z. M., & Blikslager, A. T., 2020. The integral role of tight junction proteins in the repair  
556 of injured intestinal epithelium. *International Journal of Molecular Sciences*, 21.

557 Teng, P. Y., Yadav, S., Castro, F. L. de S., Tompkins, Y. H., Fuller, A. L., & Kim, W. K., 2020.  
558 Graded *Eimeria* challenge linearly regulated growth performance, dynamic change of  
559 gastrointestinal permeability, apparent ileal digestibility, intestinal morphology, and tight  
560 junctions of broiler chickens. *Poultry Science*, 99, 4203–4216.

561 Teng, P. Y., Choi, J., Tompkins, Y., Lillehoj, H., Kim, W., 2021. Impacts of increasing challenge  
562 with *Eimeria maxima* on the growth performance and gene expression of biomarkers  
563 associated with intestinal integrity and nutrient transporters. *Vet Res*, 52, 81.

564 Van Itallie, C. M., & Anderson, J. M., 2006. Claudins and epithelial paracellular transport.  
565 *Annual Review of Physiology*, 68, 403–429.

566 Van Itallie, C. M., Fanning, A. S., Holmes, J., & Anderson, J. M., 2010. Occludin is required for  
567 cytokine-induced regulation of tight junction barriers. *J of Cell Science*, 123, 2844–2852.

1  
2  
3  
4  
5  
6  
7  
8  
9  
10  
11  
12  
13  
14  
15  
16  
17  
18  
19  
20  
21  
22  
23  
24  
25  
26  
27  
28  
29  
30  
31  
32  
33  
34  
35  
36  
37  
38  
39  
40  
41  
42  
43  
44  
45  
46  
47  
48  
49  
50  
51  
52  
53  
54  
55  
56  
57  
58  
59  
60  
61  
62  
63  
64  
65

568 Wada, M., Tamura, A., Takahashi, N., & Tsukita, S., 2013. Loss of claudins 2 and 15 from mice  
569 causes defects in paracellular Na<sup>+</sup> flow and nutrient transport in gut and leads to death from  
570 malnutrition. *Gastroenterology*, 144, 369–380.

571 Withanage, G. S. K., Kaiser, P., Wigley, P., Powers, C., Mastroeni, P., Brooks, H., Barrow, P.,  
572 Smith, A., Maskell, D., & McConnell, I., 2004. Rapid Expression of Chemokines and  
573 Proinflammatory Cytokines in Newly Hatched Chickens Infected with *Salmonella enterica*  
574 Serovar Typhimurium. *Infection and Immunity*, 72, 2152–2159.

575 Willemsen, L. E. M., Hoetjes, J. P., Van Deventer, S. J. H., & Van Tol, E. A. F., 2005.  
576 Abrogation of IFN- $\gamma$  mediated epithelial barrier disruption by serine protease inhibition.  
577 *Clinical Experimental Immunology*, 142, 275–284.

578 Wolk, K., Witte, E., Wallace, E., Döcke, W.D., Kunz, S., Asadullah, K., Volk, H.D., Sterry, W.,  
579 & Sabat, R., 2006. IL-22 regulates the expression of genes responsible for antimicrobial  
580 defense, cellular differentiation, and mobility in keratinocytes: a potential role in psoriasis.  
581 *European Journal of Immunology*, 36.

582 Ye, D., & Ma, T. Y., 2008. Cellular and molecular mechanisms that mediate basal and tumor  
583 necrosis factor- $\alpha$  induced regulation of myosin light chain kinase gene activity. *J Cell Mol*  
584 *Med*, 12, 1331–1346.

585 Zhou, B., Jia, L., Wei, S., Ding, H., Yang, J., Wang, H., 2020. Effects of *Eimeria tenella*  
586 infection on the barrier damage and microbiota diversity of chicken cecum, *Poultry Science*,  
587 99, 1297-1305.

1  
2  
3  
4  
5  
6  
7  
8  
9  
10  
11  
12  
13  
14  
15  
16  
17  
18  
19  
20  
21  
22  
23  
24  
25  
26  
27  
28  
29  
30  
31  
32  
33  
34  
35  
36  
37  
38  
39  
40  
41  
42  
43  
44  
45  
46  
47  
48  
49  
50  
51  
52  
53  
54  
55  
56  
57  
58  
59  
60  
61  
62  
63  
64  
65

**588 Table caption**

**589 Table 1.** The scoring system for evaluating inflammation level.

**590**

**591 Table 2.** The sequence of primer pairs used for amplification of target genes. Note: RPS17

**592** (Ribosomal protein S17); JAM-2 (Junctional adhesion molecule 2); ZO-1 (Zonula occludins 1);

**593** E-cadherin (Epithelial cadherin); IL (Interleukin); TNF- $\alpha$  (Tumor necrosis factor- $\alpha$ ); IFN- $\gamma$

**594** (Interferon  $\gamma$ ).

**595**

**596 Table 3.** Feces observation and histomorphology lesion score evaluation.

1  
2  
3  
4  
5  
6  
7  
8  
9  
10  
11  
12  
13  
14  
15  
16  
17  
18  
19  
20  
21  
22  
23  
24  
25  
26  
27  
28  
29  
30  
31  
32  
33  
34  
35  
36  
37  
38  
39  
40  
41  
42  
43  
44  
45  
46  
47  
48  
49  
50  
51  
52  
53  
54  
55  
56  
57  
58  
59  
60  
61  
62  
63  
64  
65

597 **Figure legends**

598 **Figure 1.** Fecal oocyst shedding was monitored daily from 5 to 10 days post-infection (dpi).

599 Error bars represent the standard error of the mean (SEM).

600

601 **Figure 2.** Histopathology of HE-stained cecum sections. HE-stained specimens were observed  
602 under light microscopy. Arrows indicate the infiltrating immune cells. Arrowheads indicate the  
603 epithelial layer. (A) Three dpi. Magnitude is  $\times 200$ ; (B) Four dpi. Magnitude is  $\times 200$ ; (C) Five  
604 dpi. Magnitude is  $\times 200$ ; (D) Six dpi. Magnitude is  $\times 200$ .

605

606 **Figure 3.** The concentration of FITC-d in the plasma of chicken, data are expressed as mean  $\pm$   
607 standard error of the mean. FITC-d (2.2 mg/ml) was administered by oral gavage 2.5 h before  
608 blood sample collection. <sup>a, b, c</sup> different superscripts show the significance between the days at  $P$   
609  $< 0.05$ .

610

611 **Figure 4.** The mRNA expression levels of claudins in ceca of chicken with *E. tenella*. Control  
612 group, chicks in this group were not treated as a control; *E. tenella*-infected group, chicks in this  
613 group were orally infected with  $1 \times 10^4$  oocysts of *E. tenella*. The open column represents the  
614 control group. The filled column represents the *E. tenella*-infected group. Amplifications were  
615 performed on three independent samples with triplicate reactions carried out for each sample.  
616 The relative mRNA level was calculated using the  $2^{-\Delta\Delta Ct}$  method. All data are represented as the  
617 mean  $\pm$  SEM and analyzed with a one-way ANOVA with Tukey's multiple comparison test  
618 using SPSS 20.0 software. (\*:  $P < 0.05$ ; \*\*:  $P < 0.01$ ).



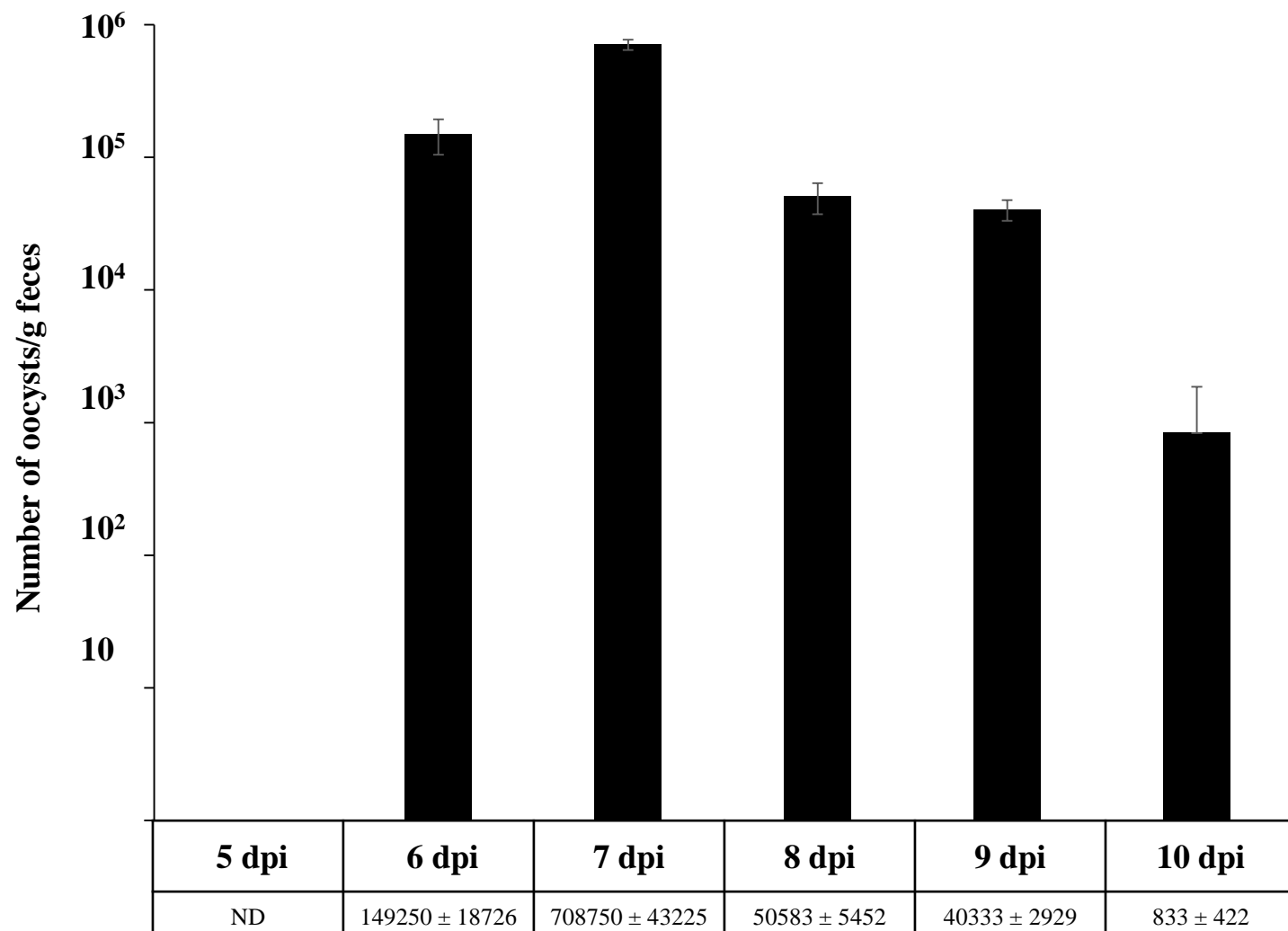
1  
2  
3  
4  
5  
6  
7  
8  
9  
10  
11  
12  
13  
14  
15  
16  
17  
18  
19  
20  
21  
22  
23  
24  
25  
26  
27  
28  
29  
30  
31  
32  
33  
34  
35  
36  
37  
38  
39  
40  
41  
42  
43  
44  
45  
46  
47  
48  
49  
50  
51  
52  
53  
54  
55  
56  
57  
58  
59  
60  
61  
62  
63  
64  
65

619  
620  
621  
622  
623  
624  
625  
626  
627  
628

**Figure 5.** The mRNA expression levels of Occludin, ZO-1, E-cadherin, and JAM-2 in ceca of chicken with *E. tenella*. Control group, chicks in this group were not treated as a control; *E. tenella*-infected group, chicks in this group were orally infected with  $1 \times 10^4$  oocysts of *E. tenella*. The open column represents the control group. The filled column represents the *E. tenella*-infected group. Amplifications were performed on three independent samples with triplicate reactions carried out for each sample. The relative mRNA level was calculated using the  $2^{-\Delta\Delta C_t}$  method. All data are represented as the mean  $\pm$  SEM and analyzed with a one-way ANOVA with Tukey's multiple comparison test using SPSS 20.0 software. (\*:  $P < 0.05$ ; \*\*:  $P < 0.01$ ).

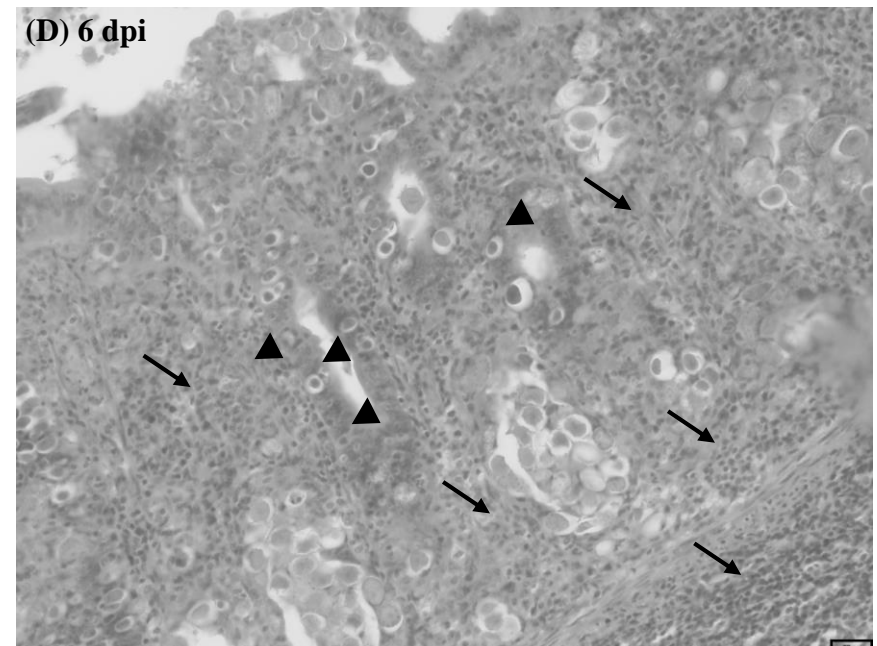
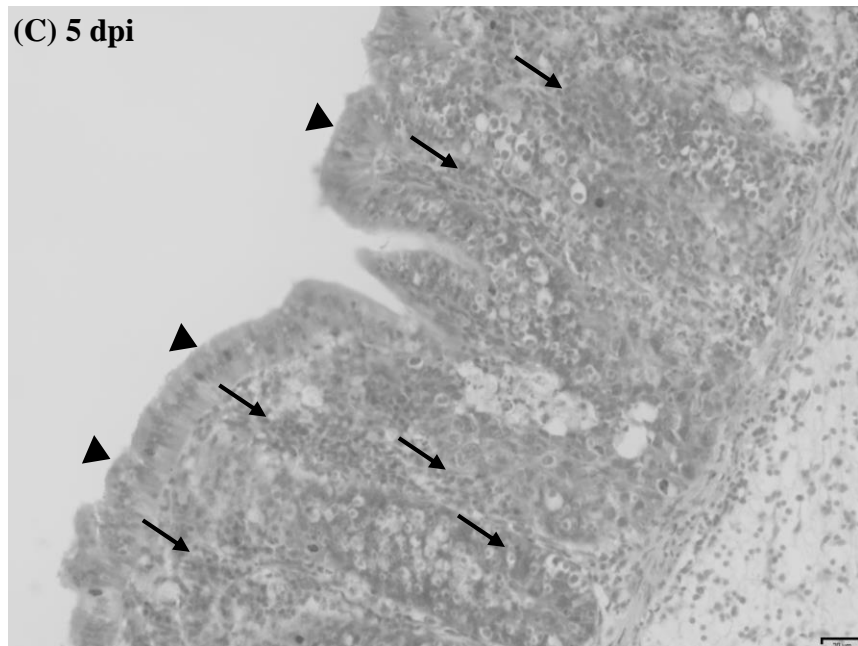
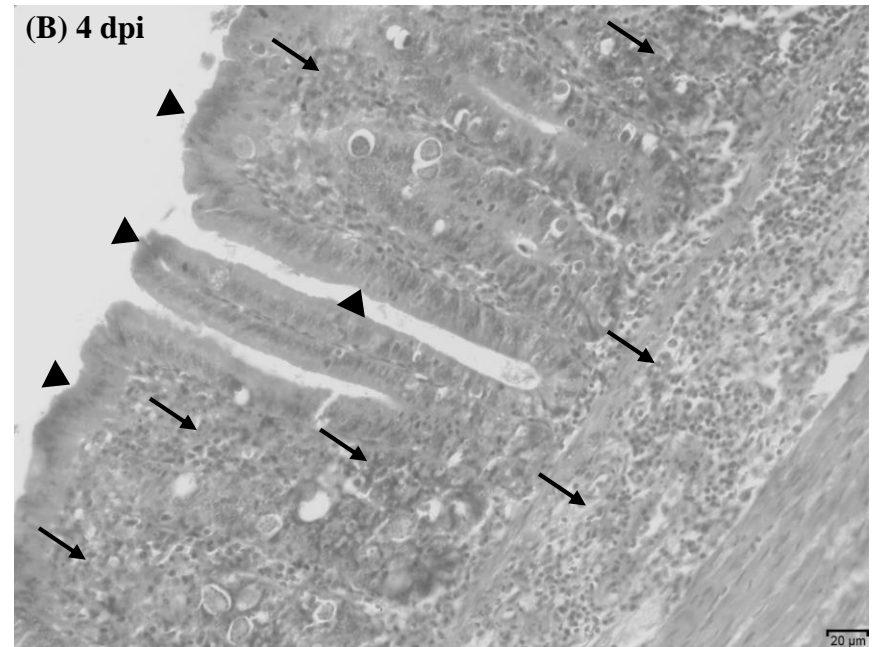
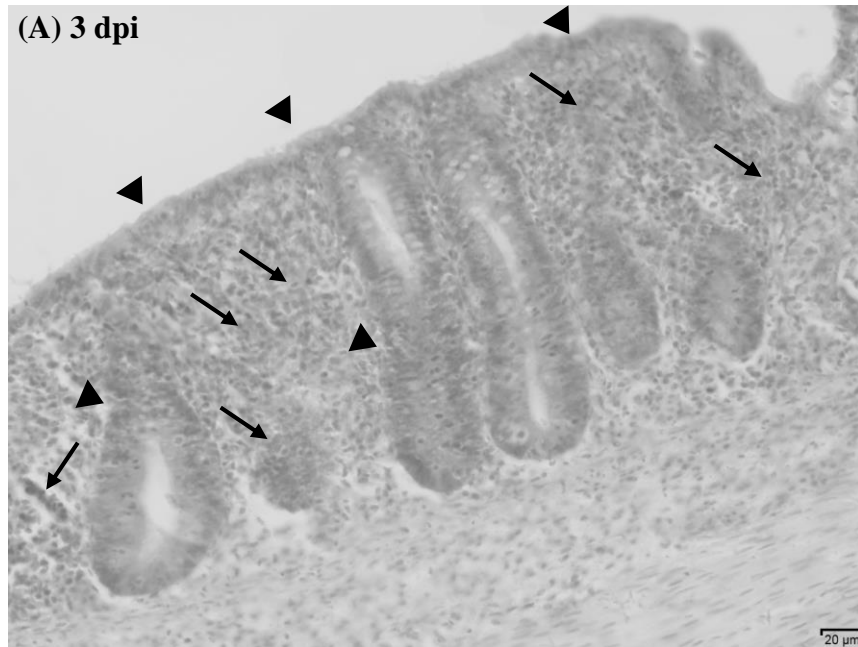
629  
630  
631  
632  
633  
634  
635  
636  
637

**Figure 6.** The mRNA expression levels of Cytokine in ceca of chicken with *E. tenella*. Control group, chicks in this group were not treated as a control; *E. tenella*-infected group, chicks in this group were orally infected with  $1 \times 10^4$  oocysts of *E. tenella*. The open column represents the control group. The filled column represents the *E. tenella*-infected group. Amplifications were performed on three independent samples with triplicate reactions carried out for each sample. The relative mRNA level was calculated using the  $2^{-\Delta\Delta C_t}$  method. All data are represented as the mean  $\pm$  SEM and analyzed with a one-way ANOVA with Tukey's multiple comparison test using SPSS 20.0 software. (\*:  $P < 0.05$ ).

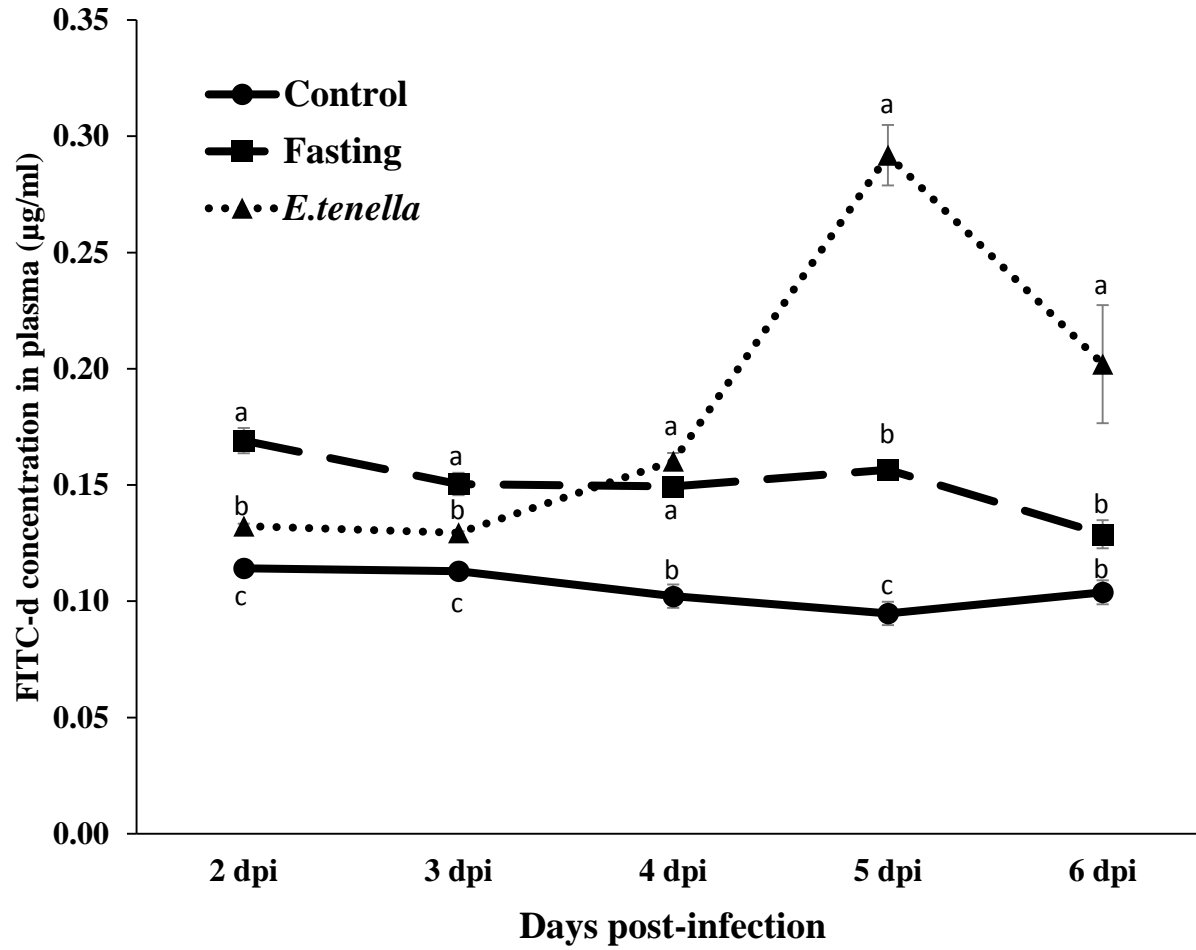
**Hung HSP et al., Fig. 1**

ND: Not detected

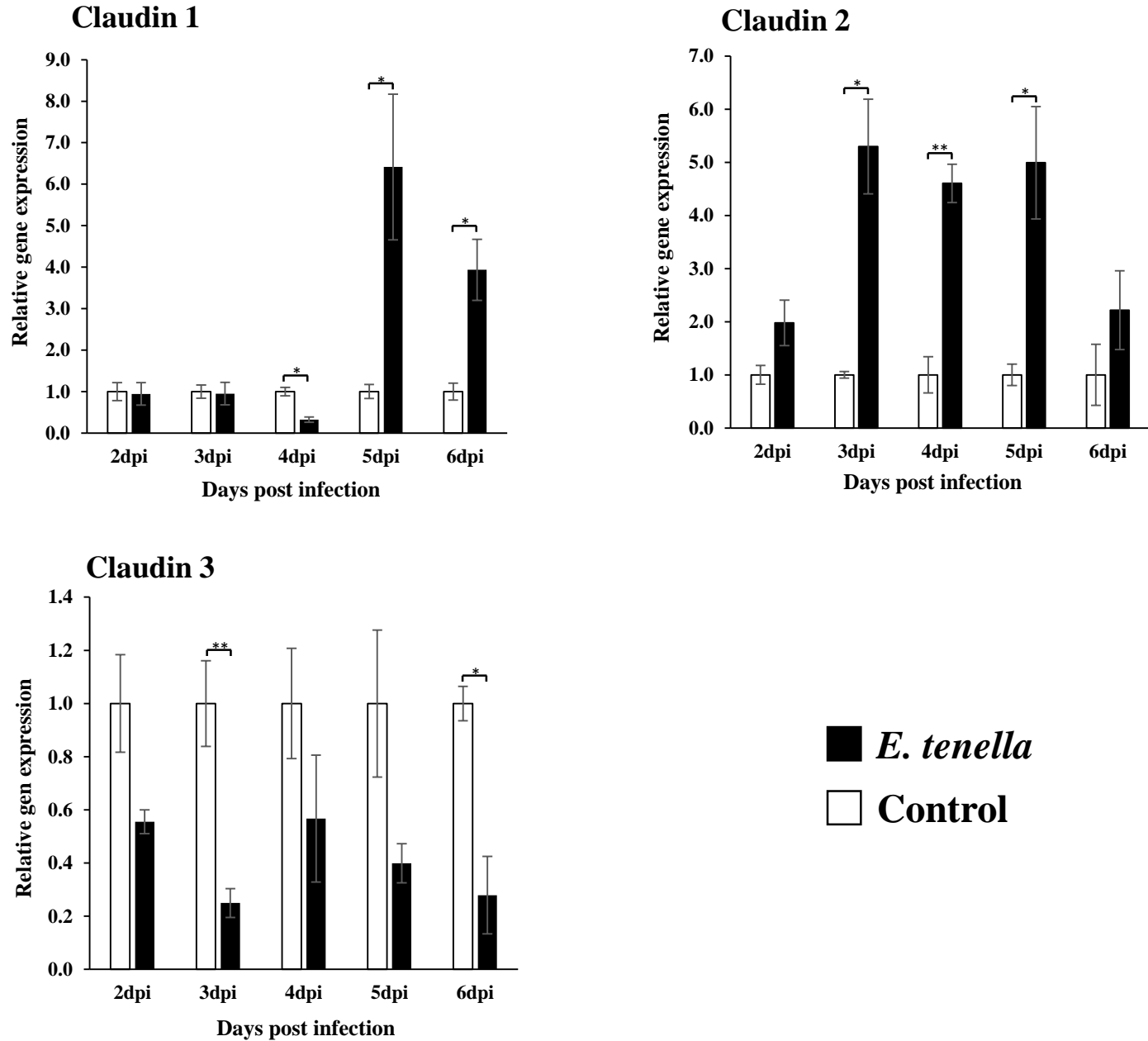
## Hung HSP et al., Fig. 2



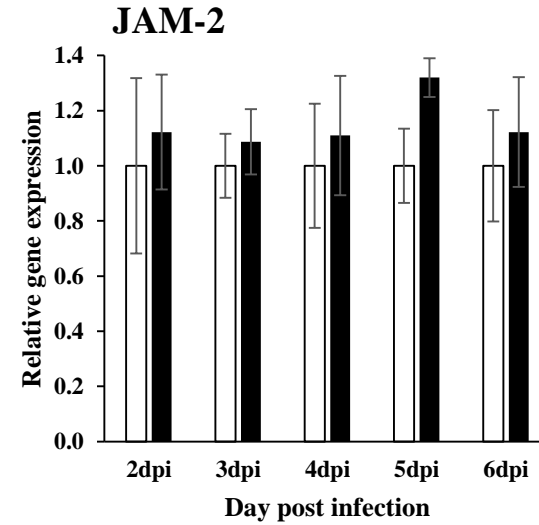
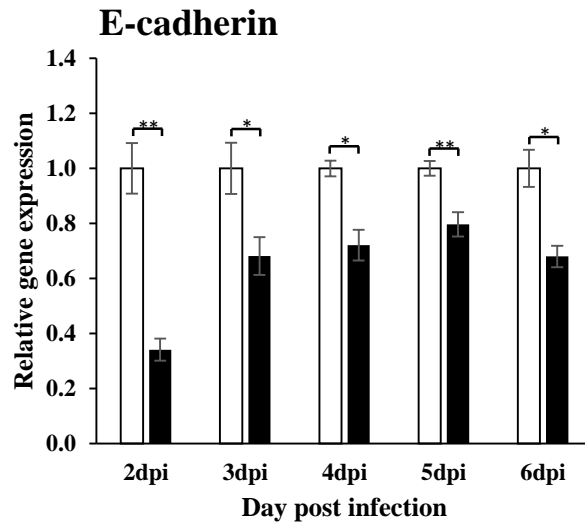
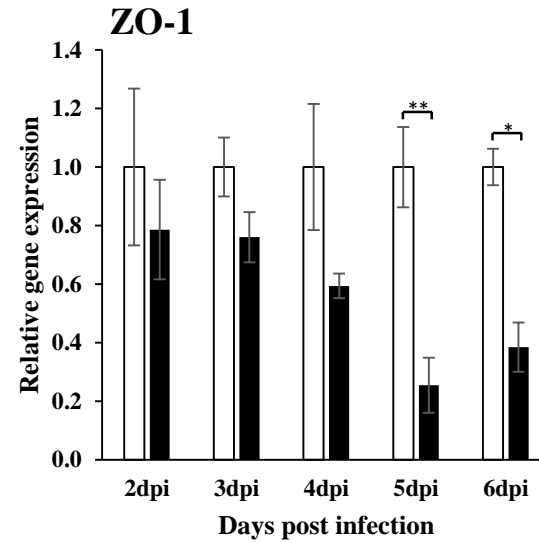
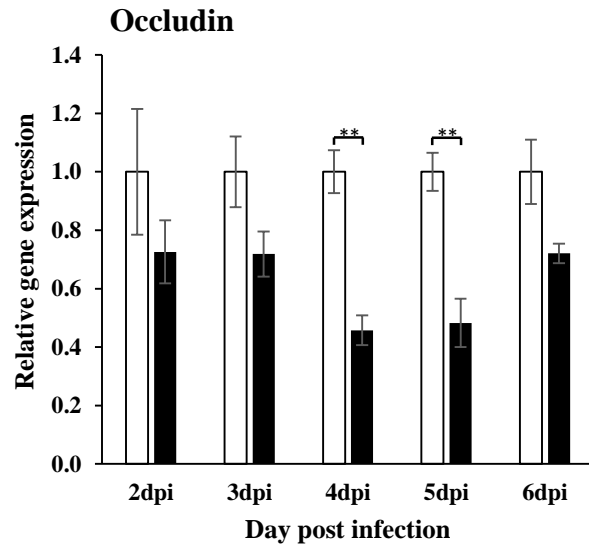
Hung HSP et al., Fig. 3



Hung HSP et al., Fig. 4

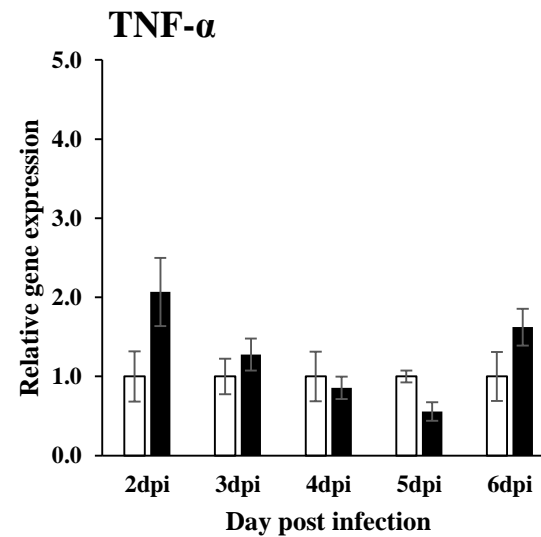
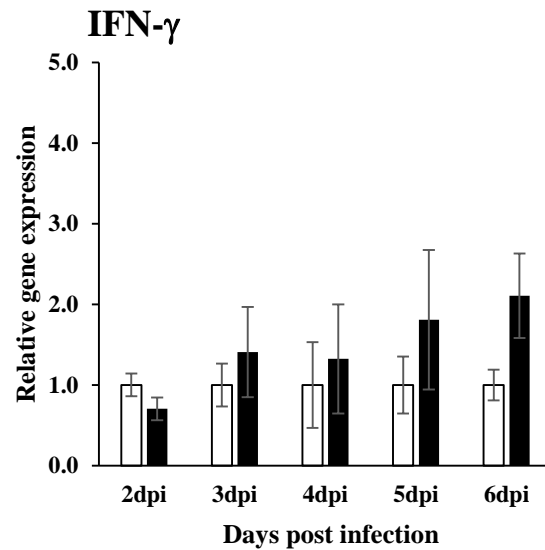
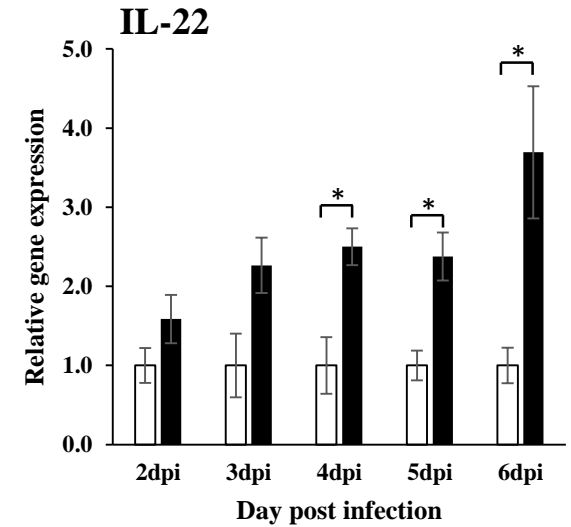
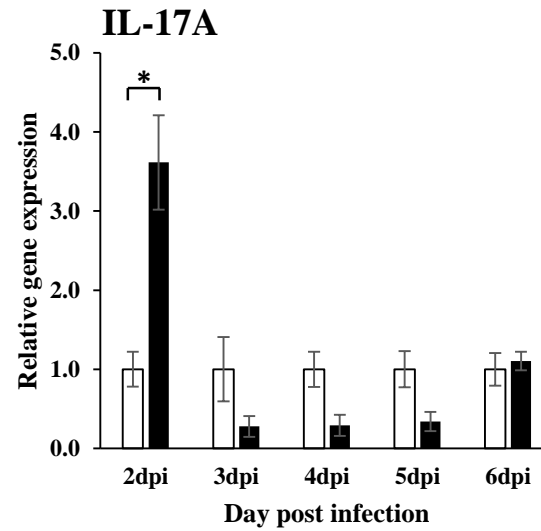
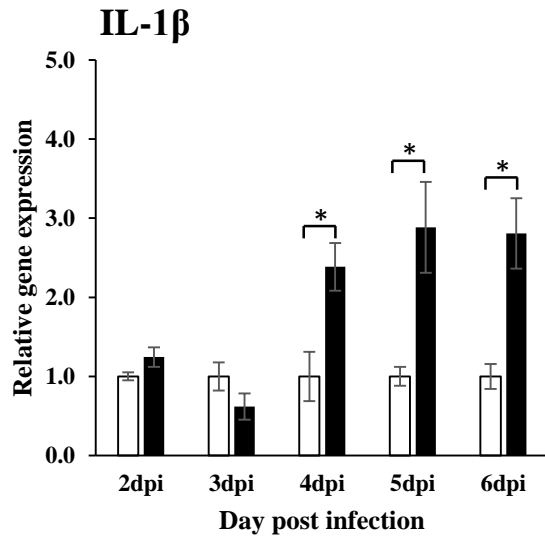


# Hung HSP et al., Fig. 5



■ *E. tenella*  
□ Control

# Hung HSP et al., Fig. 6



■ *E. tenella*  
□ Control

**Table 1.** The scoring system for evaluating inflammation level.

| <b>Inflammatory cell infiltration</b> |   | <b>Epithelial changes</b> | <b>Mucosal architecture</b> | <b>Score</b> |
|---------------------------------------|---|---------------------------|-----------------------------|--------------|
| <b>Severity</b>                       | <b>Extent</b>                           |                           |                             |              |
| Minimal                               | Mucosa                                  | Minimal Hyperplasia       |                             | 1            |
| Mild                                  | Mucosa and submucosa                    | Mild Hyperplasia          |                             | 2            |
| Moderate                              | Mucosa, submucosa, sometimes transmural | Moderate Hyperplasia      |                             | 3            |
| Marked                                | Mucosa, submucosa, often transmural     | Marked Hyperplasia        | Ulceration, Crypt loss      | 4            |



**Table 2.** The sequence of primer pairs used for amplification of target genes.

| Gene Name                   | Primer sequence (5' to 3') |                          | Accession No.  |
|-----------------------------|----------------------------|--------------------------|----------------|
|                             | Forward                    | Reverse                  |                |
| <b>Junctional Molecules</b> |                            |                          |                |
| Caludin-1                   | AAGGTGTACGACTCGCTGCT       | CAGCAACAAACACACCAACC     | NM_001013611.2 |
| Caludin-2                   | CCTGCTCACCCCTCATTGGAG      | GCTGAACTCACTCTTGGGCT     | NM_001277622.1 |
| Caludin-3                   | GCCAAGATCACCATCGTCTC       | CACCAGCGGGTTGTAGAAAT     | NM_204202.1    |
| Occludin                    | ACGGCAAAGCCAACATCTAC       | ATCCGCCACGTTCTTCAC       | NM_205128.1    |
| ZO-1                        | AAGTGGGAAGAATGCCAAAA       | GGTCCTTGGATCCCGTATCT     | XM_015278981.2 |
| JAM-2                       | AGACAGGAACAGGCAGTGCT       | TCCAATCCCATTGAGGCTA      | XM_025149444.1 |
| E-cadherin                  | TCACGGGCAGATTTCTAT         | CACGGAGTTCGGAGTTTA       | NM_001039258.2 |
| <b>Cytokines</b>            |                            |                          |                |
| IL-1 $\beta$                | GTACCGAGTACAACCCCTGC       | AGCAACGGGACGGTAATGAA     | NM_204524.1    |
| IL-17A                      | CATGGGATTACAGGATCGATGA     | GCGGCACTGGGCATCA         | NM_204460.1    |
| IL-22                       | TCAACTTCCAGCAGCCCTACAT     | TGATCTGAGAGCCTGGCCATT    | XM_025147965.1 |
| TNF- $\alpha$               | GGCGGTGCGGCCATATAA         | ATTGACGTCGTTCTGAGCGG     | MF_000729.1    |
| IFN- $\gamma$               | AAGTCAAAGCCGCACATCAAAC     | CTGGATTCTCAAGTCGTTTCATCG | NM_205149.1    |
| <b>Internal control</b>     |                            |                          |                |
| RPS17                       | AAGCTGCAGGAGGAGGAGAGG      | GGTTGGACAGGCTGCCGAAGT    | NM_204217.1    |

**Table 3.** Feces observation and histomorphology lesion score evaluation.

| <b>Day post infection</b> |                 | <b>1</b> | <b>2</b>          | <b>3</b>          | <b>4</b>          | <b>5</b>         | <b>6</b>          | <b>7</b>          | <b>8</b>          | <b>9</b> | <b>10</b> |
|---------------------------|-----------------|----------|-------------------|-------------------|-------------------|------------------|-------------------|-------------------|-------------------|----------|-----------|
| <b>Symptoms</b>           | <b>Diarrhea</b> | -        | -                 | +                 | +                 | +                | +                 | +                 | +                 | -        | -         |
|                           | <b>Blooding</b> | -        | -                 | -                 | +                 | +                | +                 | -                 | -                 | -        | -         |
| <b>Lesion score</b>       | <b>Mean</b>     | ND       | 0.83 <sup>a</sup> | 1.22 <sup>a</sup> | 2.44 <sup>b</sup> | 3.5 <sup>c</sup> | 3.56 <sup>c</sup> | 3.78 <sup>c</sup> | 3.67 <sup>c</sup> | ND       | ND        |
|                           | <b>± SEM</b>    |          | ± 0.17            | ± 0.11            | ± 0.22            | ± 0.10           | ± 0.11            | ± 0.11            | ± 0.19            |          |           |